EMTP Modeling of Cogeneration System for Transient Stability Analysis

Wei-Neng Chang, Chia-Han Hsu

***Abstract*—** This paper focuses on the EMTP modeling of a cogeneration system for transient stability analysis. First, the structure and operation mode of the cogeneration system are introduced. Then, use of the electromagnetic transient program (EMTP) constructs the overall cogeneration system. The effects of unbalanced faults on the transient stability of the cogeneration system are observed with the modeled system. Several fault types, including 3-line-to-ground (3LG) fault, double line-to-ground (2LG) fault, line-to-line fault (2LF), and single line-to-ground (SLG) fault are assigned respectively for transient stability simulations. Finally, use of critical clearing time (CCT) curves evaluate the transient stability of the cogeneration system to different types of short-circuit faults. The simulation results are listed and evaluated.

***Keywords*—** CCT curve, EMTP, Transient stability, Unbalanced faults.

I. Introduction

Due to high utilization ratio of energy, cogeneration systems, or called "combined heat and power (CHP) systems," are widely employed in the world for industrial processes. A cogeneration plant is composed of cogenerators and in-plant process loads. Usually, cogeneration system is operated in parallel with utility for improvement of operational reliability. When short-circuit faults occur in the utility side, voltage sags will spread and penetrate into cogeneration plant [1]~[4]. Different types of short-circuit fault generate different degrees of voltage sage. Severe voltage sages with long enough fault intervals may cause cogenerators in the plant out-of-step [5]~[7]. Before lose-of-synchronism, the cogeneration plant should be disconnected from the utility grid and operated alone to prevent these cogenerators in the plant from out-of-step. Use of CCT curves can evaluate the transient stability of the cogenerators to the short-circuit faults. Under voltage relay (27) with directional over-current relay (67) can be used together to identify the faults occurring in the utility [8]~[9]. Grid-disconnection operation should be executed according to the CCT curves to keep the plant be operated safely. This enhances the fault-ride-through ability of the plant.

Manuscript received October 21, 2011;

Wei-Neng Chang is with the Department of Electrical Engineering, Chang Gung University, 259 Wen-Hwa 1st Road, Kwei-Shan, Tao-Yuan, Taiwan, ROC. (e-mail: nchang@mail.cgu.edu.tw)

Due to calculation limitations of simulation programs, balance three-phase faults are usually assigned for transient stability analysis of power systems. However, most faults that frequently occur in power systems are unbalanced faults. The influence of unbalanced faults to cogeneration system needs to be clarified. This helps the field engineers in the cogeneration plant to realize their power system more widely and also helps then to establish suitable protection system, such as settings of protection relays and relative parameters for necessary grid-disconnection schemes, to protect cogeneration units from out-of-synchronism.

Since 1970s, the EMTP program has been widely used in power industries for transient phenomena analyses. Since multi-phase structure is used in the EMTP, the EMTP program can be employed for unbalanced operation analysis as well. With a friendly graphic user interface (GUI) introduced in the modern EMTP program, users can model the studied system easily for analysis [10]. In the paper, the cogeneration system is constructed in the EMTP environment for transient stability analysis. This paper observes the effects of unbalanced faults on the transient stability of a real cogeneration plant. For the need of unbalanced operations, the EMTP program is employed in the paper. For comparisons, transient stability analysis with 3LG fault is firstly conducted as a base case. Then EMTP simulations with different types of faults are performed. The simulation results are listed and compared.

II. Cogeneration System Structure

Fig. 1 shows the single-line diagram of a real cogeneration system to be studied in the paper. Four coal-fired cogeneration units are installed in the plant. The cogenerators in the plant generate steam and electricity at the same time. The generated steam offers heat source for the needs of the manufacturing processes in the plant. The electricity outputs of the cogenerators supply the load demands in the plant. In addition, the remaining power is exported to the utility. Hence, the plant is an exporting type cogeneration plant. Table I shows the cogenerators' specifications. Table II lists the basic power flow of the plant for transient stability evaluations. The total electricity generation of the plant is 307MW in the peak load period and 193MW in the off-peak load period of the utility. The total load demand in the plant is kept at a constant of 180MW. During the peak load period, the cogeneration plant sells electricity to the utility. During the off-peak period, the electricity output of the cogeneration plant is reduced to nearly zero.

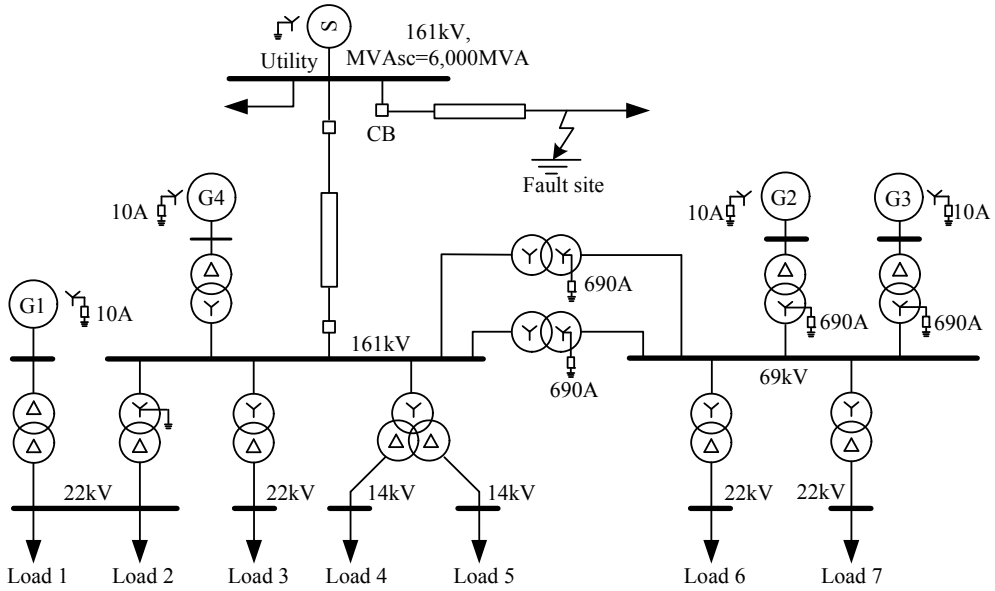

Fig. 1 single-line diagram of the cogeneration system

TABLE 1
RATED PARAMETERS OF COGENERATOR UNITS

	capacity (MVA)	voltage (kV)	H (Sec)	pf
G1	62.4	11	1.94	0.8
G2	125.9	11	2.69	0.8
G3	125.9	11	2.69	0.8
G4	157.4	11	2.81	0.8

TABLE 2
BASIC POWER FLOW OF THE SYSTEM

		voltage(kV)	utility load condition	(MW)
Cogenerator units	G1	22	peak load	37
			off-peak load	23
	G2	69	peak load	83
			off-peak load	53
	G3	69	peak load	92.2
			off –peak load	62.2
	G4	161	peak load	94.5
			off-peak load	54.5
Load demands(MW)	Load 1	22	30	
	Load 2	22	45	
	Load 3	22	32	
	Load 4	14	13	
	Load 5	14	20	
	Load 6	22	16	
	Load 7	22	24	

All the cogeneration units in the plant are equipped with voltage control systems and power control systems. The voltage control system in a generator usually composes of automatic voltage controller (AVR) and exciter. On the other hand, the power control system in a generator has governor and turbine system. IEEE standards offer standard block diagrams of the voltage and power control systems for computer simulations [11]~[12]. Fig. 2(a) shows the IEEE-AC1 brushless excitation system and Fig. 2(b) shows the IEEE-ST2 steam turbine/governor system for all cogeneration units in the plant. Before simulations, Fig. 2(a) and (b) should be built in the EMTP environment.

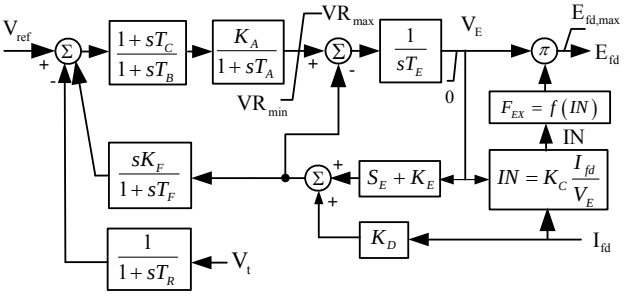

(a) IEEE-AC1 voltage control system

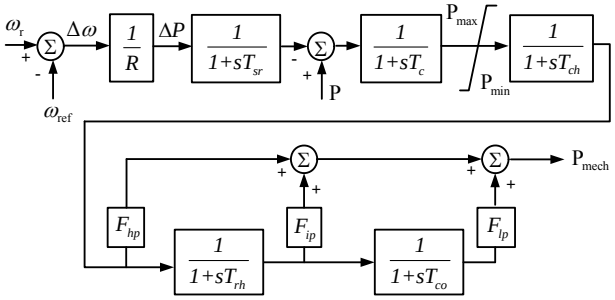

(b) IEEE-ST2 power control system

Fig. 2 IEEE standard voltage and power control block diagrams for the cogeneration units

The loads in the plant are considered as composite loads, which include static load and dynamic load. Generally, static load represents load as a combination of passive elements, such as resistor, capacitor, and reactor. Heaters and lighting facilities are static load. Dynamic load model is used for motor loads. Since the cogeneration plant has powerhouses and chemical processes which use heaters and induction motor loads, dynamic and static loads are modeled for the plant. Fig. 3 shows the load model for the plant.

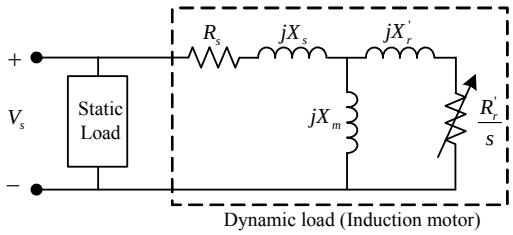

Fig. 3 the load model for the plant

Equation (1) shows the rotor dynamics of the induction motor in the dynamic load. Equation (2) represents the load torque-speed characteristic of the motor load.

$$M\frac{d\omega_r}{dt}+D\omega_r=T_E-T_L \quad (1)$$

$$T_L(\omega_r)=-1.47\omega_r^3+3.21\omega_r^2-0.91\omega_r+0.1 \quad (2)$$

In which: M =inertia constant of motor and load,
D =damping factor,
ω_r =speed, T_E =induced torque,
T_L =load torque.

Generally, static loads can be represented as (3) and (4), called ZIP load model [13].

$$P_L(V,f)=P_0[p_1+p_2(\frac{V}{V_0})+p_3(\frac{V}{V_0})^2](1+p_4(\frac{f}{f_0})) \quad (3)$$

$$Q_L(V,f)=Q_0[q_1+q_2(\frac{V}{V_0})+q_3(\frac{V}{V_0})^2](1+q_4(\frac{f}{f_0})) \quad (4)$$

In which: P_0, Q_0, V_0, f_0 =operating points,
$p_1 \sim p_4$, $q_1 \sim q_4$ =relative coefficients of active power and reactive power.

The Load 4 and Load 5 in the plant are represented as purely static loads, other loads are represented as 80% dynamic load and 20% static load in the simulation.

III. EMTP Modeling of the Cogeneration System

Fig. 4 shows the EMTP modeling of the subsystems of the cogeneration plant. Fig. 4(a) is the EMTP modeling of the composite load according to (1)~(4). Fig. 4(b) shows the IEEE-AC1 brushless excitation system for the voltage control subsystem of the cogenerators and Fig. 4(c) shows the IEEE-ST2 governor and steam turbine subsystem for the power control of the cogenerators, respectively. Fig. 5 shows the EMTP modeling of one of the cogeneration units. The voltage and power control systems are modeled and merged into the cogeneration unit. Fig. 6 is the EMTP modeling of the overall cogeneration plant. The transformers in the plant are also modeled in the EMTP according to manufactures' data sheets. Shorted-circuit and opened-circuit tests results for these transformers are used in the modeling.

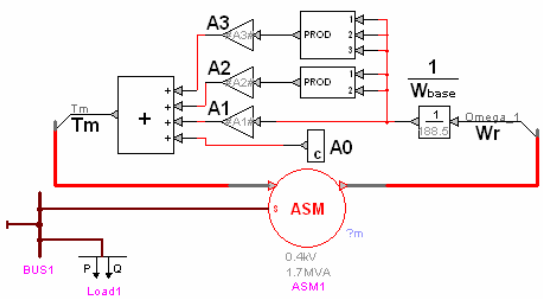

(a) the composite load

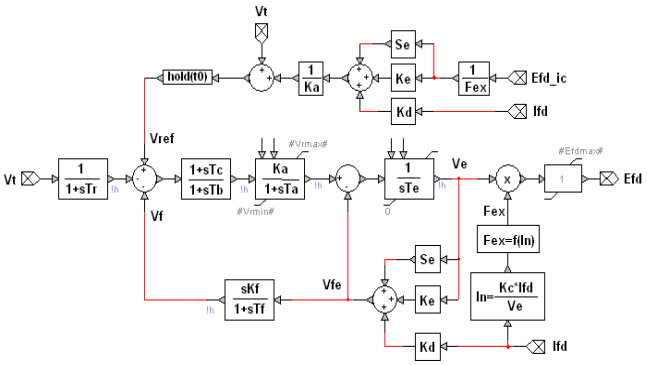

(b) the IEEE-AC1 voltage control system

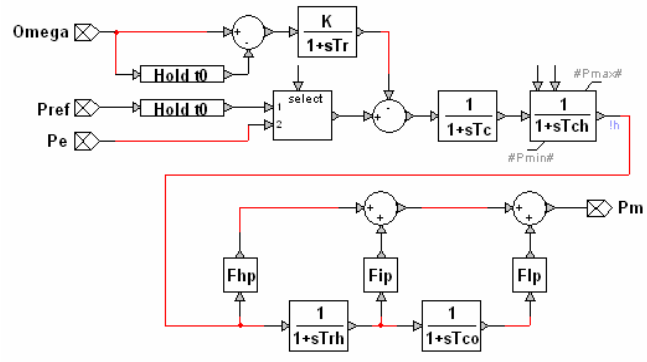

(c) the IEEE-ST2 power control system

Fig. 4 EMTP modeling of the subsystems for the cogeneration plant

The tie line between the cogeneration plant and the utility is represented as a lumped circuit. The utility is represented as a power source with a short-circuit capacity of 6,000MVA. The fault site in the utility side is modeled by using a Y-connected branch with neutral impedance to the ground. Different assigned values in the Y branch simulate different types of balance and unbalanced faults. Careful choice of impedance values in the Y branch also controls the degree of fault. For example, setting fault impedance as zero creates a complete fault. The fault residual voltage at the fault site will then be zero. Slightly increasing the fault impedance increases the fault residual voltage. With the settings, the cogeneration plant will suffer different types of fault with different fault residual voltages and fault times. This obtains the CCT curves of the cogeneration plant. Some interesting responses to the faults can then be simulated and evaluated by using the EMTP program.

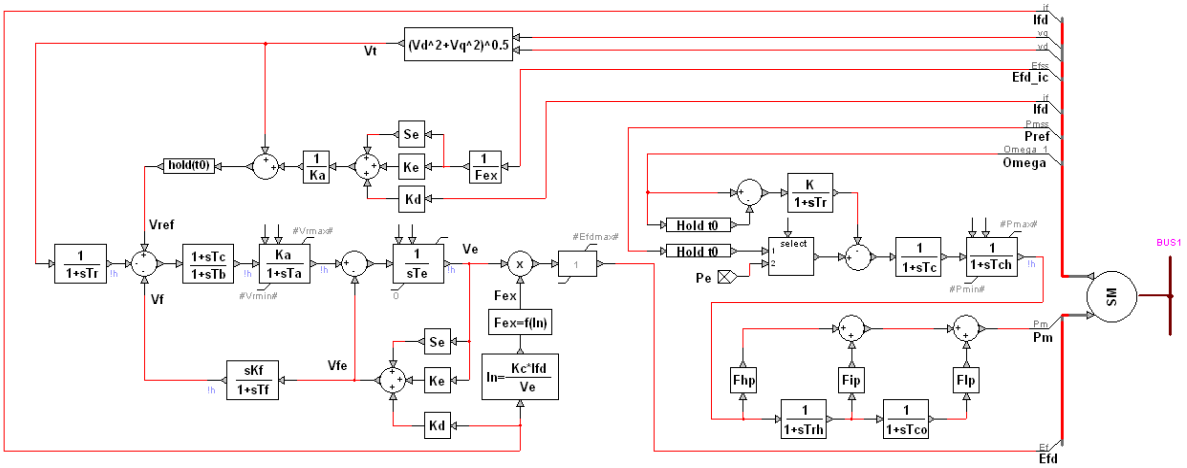

Fig. 5 EMTP modeling of one the cogeneration unit

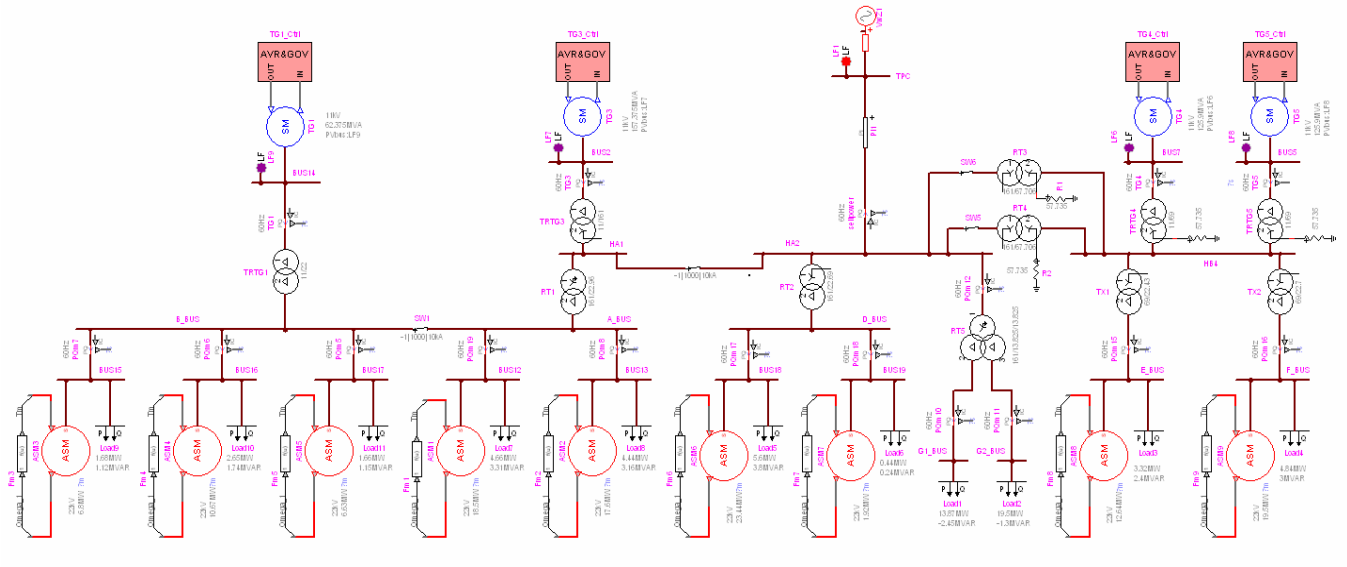

Fig. 6 EMTP modeling of the overall cogeneration plant

IV. Transient Stability Analysis

Several fault evens have been assigned in the utility for transient stability simulations of the cogeneration plant. Different fault settings with different fault impedances and fault times are assigned for the analyses to obtain the relative critical clearing time (CCT) curves. Generally, larger fault residual voltage and fault time results in longer CCT values. The assigned short-circuit faults include balance (3LG) and unbalanced faults. The paper considers the following unbalanced faults: 2LG, 2LF, and SLG faults. In the simulation, different CCT curves with different fault types for peak load and off-peak load periods are evaluated. For comparison, 3LG fault is firstly simulated as a base case.

Case 1: Base Case-3LG Fault

Fig. 7 shows the system responses for a 14 cycles complete 3LG fault occurring in the utility in the peak load period. When the fault is cleared, all the cogenerators in the plant go back to their stable operations. When the fault time is increased by an extra cycle to 15 cycles, the cogenerator G3 in the plant becomes unstable, as shown in Fig. 8. Hence, the CCT value is found to be 14 cycles.

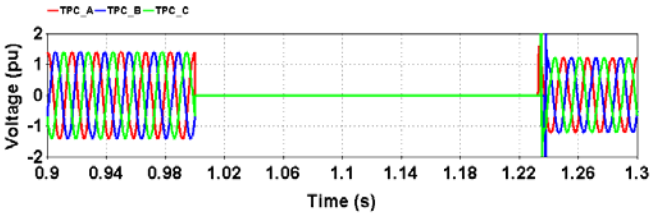

(a) fault voltage waveform in the utility

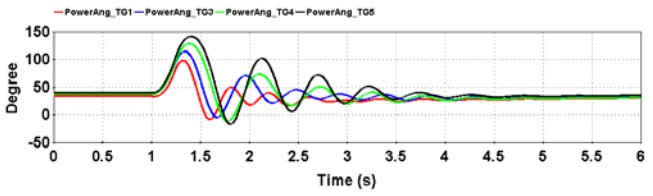

(b) rotor angle responses

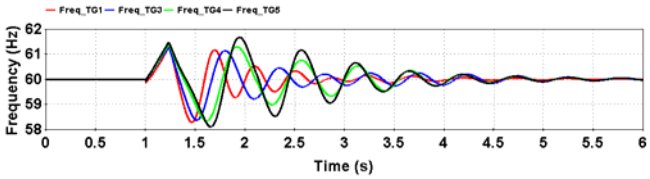

(c) frequency responses

Fig. 7 cogenerators responses to a 14 cycles (CCT), 3LG complete fault in the peak load period

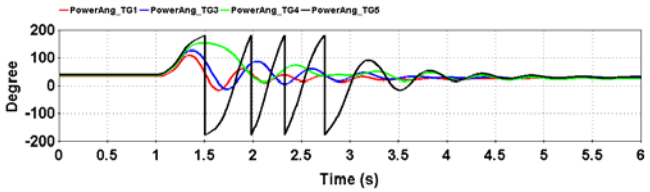

(a) rotor angle responses

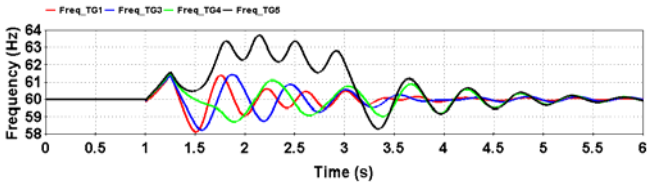

(b) frequency responses

Fig. 8 cogenerators responses to a 15 (CCT+1) cycles 3LG complete fault in the peak load period

The CCT test is also executed for the off-peak load operation period, in which all cogenerators in the plant decrease their electricity outputs, as shown in Table 2. With the setting, the total electricity output of the cogeneration plant to the utility is reduced to zero. Fig. 9 shows the simulation results. The value of CCT is extended to 21 cycles. When the fault clearing time is increased to 22 cycles, the cogenerator G3 becomes unstable, as shown in Fig. 10. It is found that although G3 and G2 are connected at the same bus and have the same structure, G3 generates more electricity then G2 in both peak load and off-peak load periods. Hence, G3 has weaker transient stability performance.

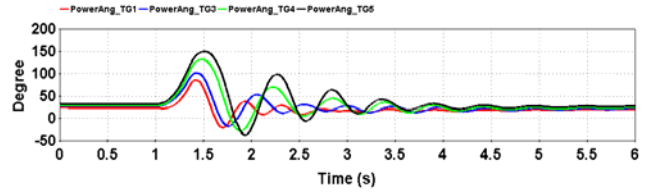

(a) rotor angles responses

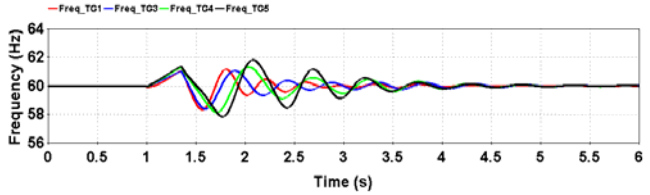

(b) frequency responses

Fig. 9 cogenerators responses to a 21 cycles 3LG fault occurring in the utility side in the off-peak load period

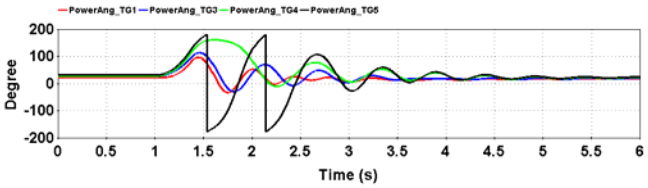

(a) rotor angle responses

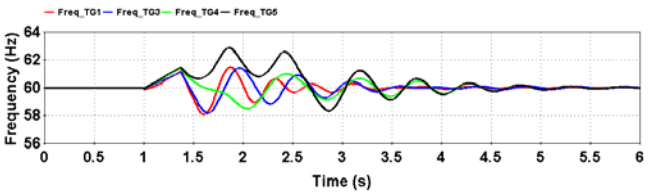

(b) frequency responses

Fig. 10 cogenerators responses to a 22 (CCT+1) cycles 3LG fault occurring in the off-peak load period

Case 2: 2LG Fault

In general, 2LG fault is the worst unbalanced fault since only one phase survives during the fault interval. In the simulation, a complete 2LG fault occurring at phase *b-c* in the utility side in the peak load period is assigned for the CCT test. Fig. 11 shows the simulation results with a fault time of 27 cycles. When the fault is cleared, all cogenerators remain stable. Fig. 12 shows the fault simulation results when the fault time is increased from 27 cycles to 28 cycles. The cogenerator G3 becomes unstable when the fault is cleared. It is concluded that the CCT is 27 cycles for a complete 2LG fault occurring in the utility side.

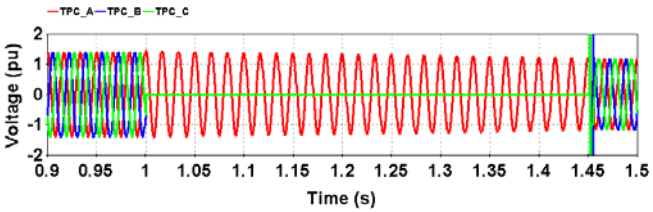

(a) fault voltage waveform in the utility

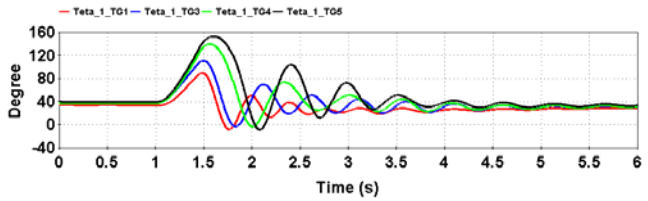

(b) rotor angle responses

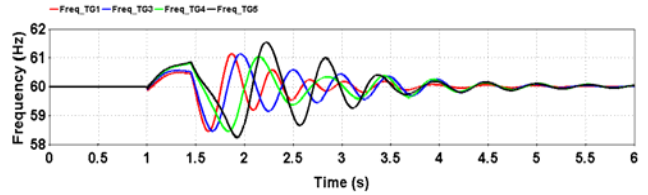

(c) frequency responses

Fig. 11 cogenerators responses to a 2LG fault with a fault time of 27 cycles (CCT) in the peak load period

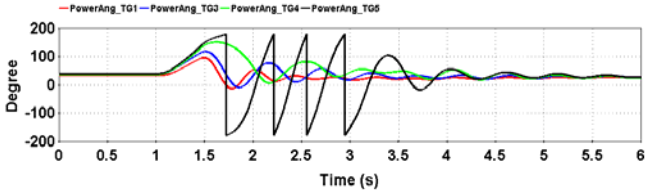

(a) rotor angle responses

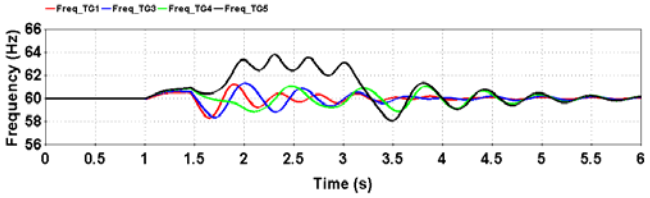

(b) frequency responses

Fig. 12 cogenerators responses to a 28 cycles (CCT+1) 2LG fault in the peak load period

Case 3: 2LF Fault

Fig. 13 shows the simulation results with an 18 cycles 2LF fault occurring at phase *b–c* in the peak load period. All the cogenerators in the plant maintain stable when the fault is celared. Further simulation shows that the CCT to the 2LF fault is over 100 cycles for both the peak load and off-peak load periods, which is long enough for protection devices to operate to clear the fault and restore the cogeneration system. The conclusion from the simulation is that the 2LF fault in the utility side does not threat the transient stability of the cogeneration plant.

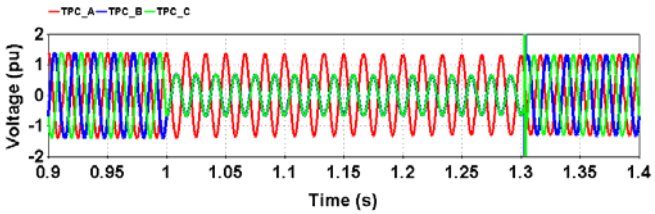

(a) fault voltage waveform in the utility

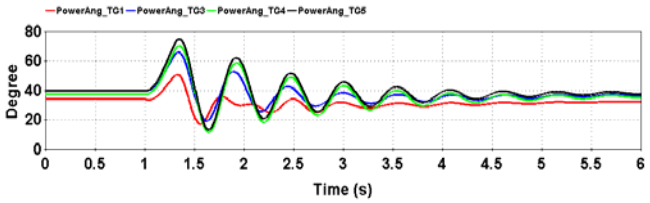

(b) rotor angle responses

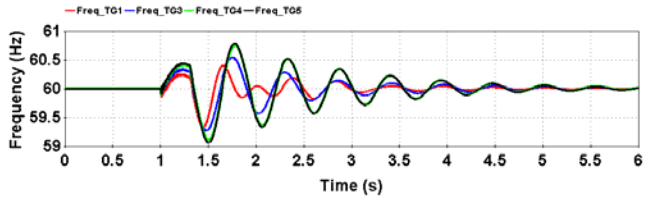

(c) frequency responses

Fig. 13 cogenerators responses to an 18 cycles 2LF fault in the peak load period

Case 4: SLG Fault

Fig. 14 shows the simulation results of a SLG fault occurring in the utility side in the peak load period. The fault time is also set at 18 cycles. The cogeneration system maintains stable when the fault is cleared. Increasing the fault time to 100 cycles does not make any of the cogenerators unstable. The simulation using the off-peak load data shows similar result. It is concluded that SLG fault in the utility hasn't significant effect on the transient stability of the cogeneration plant.

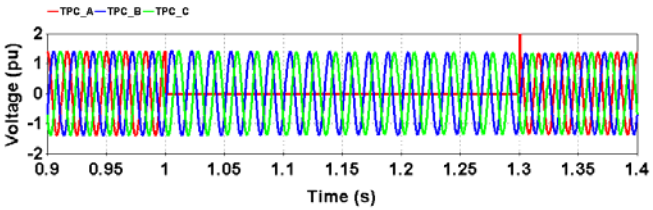

(a) fault voltage waveform in the utility

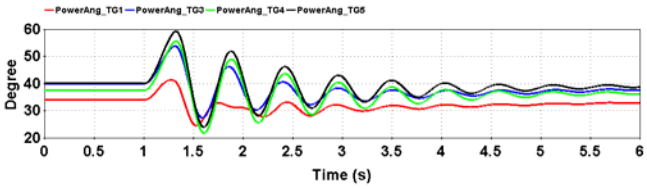

(b) rotor angle responses

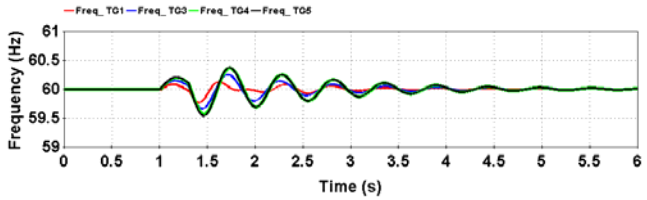

(c) frequency responses

Fig. 14 simulation result of 18 cycles SLG fault

V. Comparison of Balance and Unbalanced Faults

This section observes the effects of different types of faults on the transient stability of the cogeneration unit G3 operating in the peak load period. From the simulation results in the previous section for different faults, symmetrical components of voltages at the cogenerator G3 terminal are listed. The torque versus rotor angle characteristics of the cogenerator to different types of fault is compared. Fig. 15 shows the positive-, negative-, and zero- sequences voltage responses of G3 terminal for different types of balance and unbalanced faults. The fault times are all set at 14 cycles, which is the CCT of the G3 to 3LG fault in the utility in the peak load period. It is also observed that zero-sequence component voltage doesn't exist in all faults. This is because of the connection type of the step-up transformers used for the cogeneration units in the plant

. Fig. 15 also shows that all unbalanced faults generate negative-sequence component voltage. For the three types of fault, the 2LF fault occurring in the utility induces largest negative-sequence voltage at the G3 terminal.

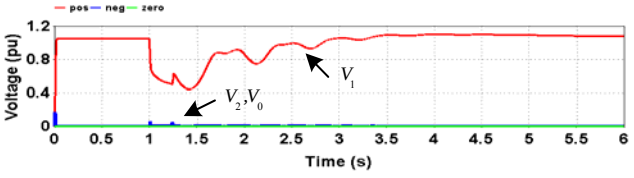

(a) 3LG fault

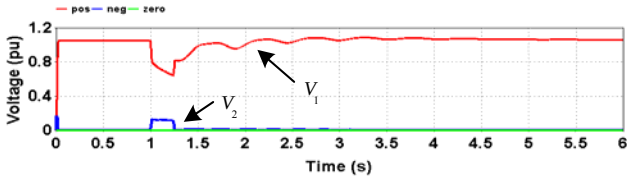

(b) 2LG fault

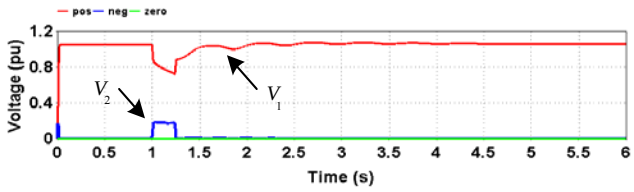

(c) 2LF fault

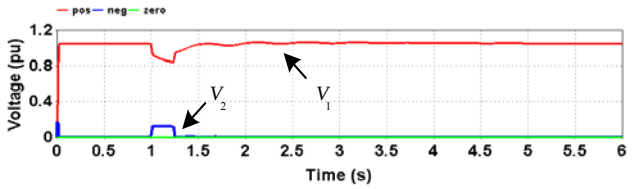

(d) SLG fault

Fig. 15 the positive-, negative-, and zero- sequences voltage responses at G3 terminal for different types of fault

Fig. 16 summarizes the torque versus rotor angle characteristics of the G3 for different types of complete faults in the peak load period. For comparison, the fault intervals are all set at 14 cycles. In the pre-fault situation, the magnetic torque of the G3 is 0.738 pu and the rotor angle is 40 degrees. Fig. 16(a) shows the torque versus rotor angle characteristics for the 14 cycles complete 3LG fault. It shows a typical oscillation phenomenon which can be widely seem in many articles describing the equal-area criteria. The fault clearing angle is 100 degrees. In the post-fault interval, the maximum rotor angle swing is 140 degrees. Fig. 16(b) shows the torque versus rotor angle characteristic for a complete 2LG fault. Fig. 15(b) shows that during the fault interval, the fault residual voltage is about 0.6 pu. The fault residual voltage partially sustains the power transfer ability of the cogenerator. The cogenerator still has power output during the fault interval. This decreases the allowable acceleration area. Hence the fault clearing angle is not so large as compared with Fig. 16(a), which leads to larger deceleration area to be used for extending the CCT value. The similar phenomena can also be observed in Fig. 16(c) and (d) for 2LF and SLG faults. It is evidenced that SLG fault hardly causes the cogenerator to be out-of-step.

The simulation results in Fig. 16 explain why the 3LG fault is the most severe fault for the transient stability performance. In addition, unbalanced faults generate negative-sequence voltages at the terminal of the cogenerator, as shown in Fig. 15. The negative-sequence voltage induces braking torque, which helps stabilizing the cogenerator from lost-of-synchronism [14]. Hence, the induced negative-sequence voltage helps increasing the CCT values.

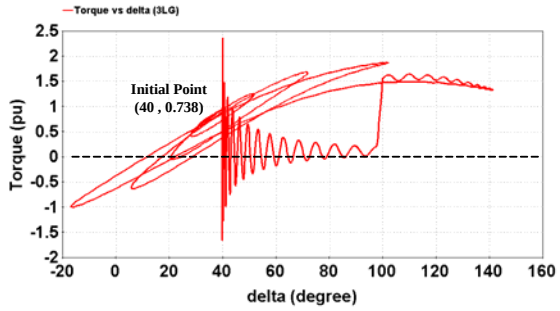

(a) 3LG fault

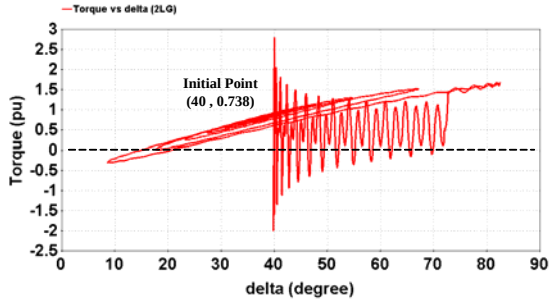

(b) 2LG fault

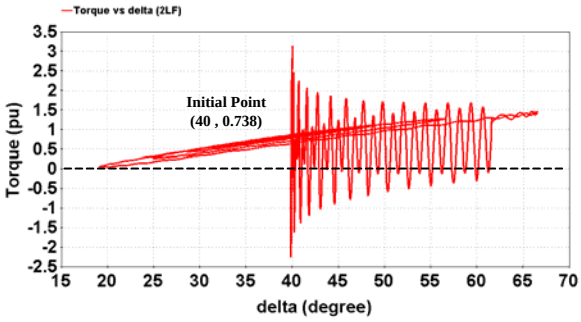

(c) 2LF fault

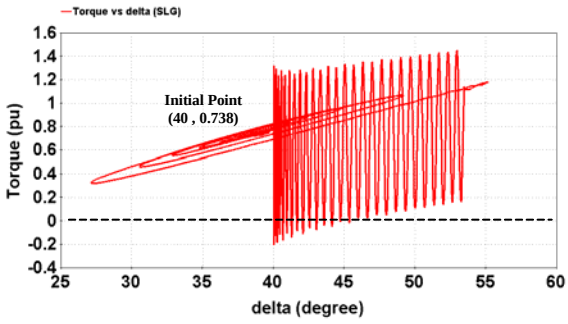

(d) SLG fault

Fig. 16 torque versus rotor angle characteristics of G3 for different types of fault

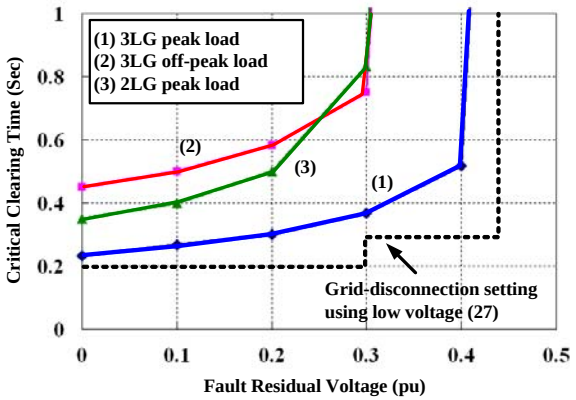

Fig. 17 the CCT curves versus fault residual voltages for different types of faults occurring in the utility

Fig. 17 summarizes the CCT curves versus fault residual voltages for the cogeneration plant for different types of faults in peak load and off-peak load periods. The CCT curves show that the cogeneration plant is most vulnerable to different degrees of 3LG fault occurring in the peak load period. The CCT curve of the 2LG fault in the peak load period lies between the 3LG faults occurring in peak load and off-peak load periods. Since the CCT values of the SLG and 2LG faults are larger than 100 ms, which can be cleared in time by protection devices, these two types of unbalanced fault are not so significant to the transient stability of the plant. Fig. 17 also recommends a low voltage tripping line for the grid-disconnection scheme of the plant. When the fault residual voltage touches the line, the plant should be disconnected from the utility and switched to islanding operation mode to protect these cogenerators in the plant.

VI. Conclusion

The paper has observed the effects of unbalanced faults on the transient stability of a real cogeneration plant by using the EMTP program. A real cogeneration system is studied. From the simulation results in the paper, the following conclusions are listed:

1. The most severe fault to the transient stability of cogeneration units is 3LG fault occurring in the peak load period for an exporting type cogeneration system.
2. When the output power of the cogeneration unit is decreased during the off-peak period, the maximum allowable swing angle is increased due to the equal-area criteria. Hence the CCT curve of the cogenerator is larger then that at the peak load period.
3. In the peak load period, the CCT curve to 2LG fault is almost twice of the CCT curve of 3LG fault. In the off-peak period, the CCT of the 2LG fault is long enough to be cleared by protection devices.
4. The SLG fault occurring in the utility is not so easy to cause cogenerator out-of-step.
5. Cogenerator with larger rotor inertia time constant will slow down the acceleration of the rotor during the fault interval. The time to critical fault clearing angle is extended.
6. Although 2LF and SLG faults are not so significant to the transient stability of the plant. When they happen, voltage sags will penetrate into the plant and cause voltage-sensitive loads to trip. This may result in the tripping of the cogenerator. The low-voltage-ride-through ability of voltage-sensitive loads in the powerhouses of the cogeneration units should be enhanced if needed.

References

[1] M. F. McGranaghan, D. R. Mueller and M. J. Samotyj, "Voltage sags in industrial systems," *IEEE Trans. Industry Applications*, vol. 29, no. 2, pp. 397-403, 1993.

[2] Y. H. Chan and C. J. Wu," Voltage sag analysis of industry power system considering CBEMA curve," *Proceedings of the 10th WSEAS/IASME International Conference on Electric Power Systems, High Voltages, Electric Machines(Power'10)*, Japan, pp.101-111, 2009.

[3] N. R. Patne and K. L. Thakre, "Fault induced voltage sag mitigation using dynamic voltage restorer," *WSEAS Trans. Power Systems*, vol. 10, no.4, pp.319~330, 2009.

[4] J. Guerrero, J. Soto, D. Robles and E. Luquez, "Study of the impact of non-rectangular voltage sags in induction motors," *Proceedings of the 8th WSEAS/IASME International Conference on Electric Power Systems, High Voltages, Electric Machines(Power'08)*, Italy, pp.172-176, 2008.

[5] J. C. Das, "Effects of momentary voltage dips on the operation of induction and synchronous motors," *IEEE Trans. Industry Applications*, vol. 26, no. 4, pp. 711-718, 1990.

[6] P. Kundur, *Power System Stability and Contro*l, Mcgraw-Hill, Inc., 1994

[7] A. Eleschova, A. Belan and M. Smitkova, "What influences length of CCT ?," *Proceedings of the 10th WSEAS/IASME International Conference on Electric Power Systems, High Voltages, Electric Machines(Power'10)*, Japan, pp.189-194, 2009.

[8] W. S. Zimmermann, S. Hopp, M. Bondeur and D. N. Chen, "Transient stability study of the Hsin Yu Co-Generation Plant in Hsin-Chu Science Based Industrial Park in Taiwan," *Proceedings of IEEE Power Engineering Society Winter Meeting*, vol. 1, pp. 452-457, 2000.

[9] C. T. Hsu, "Cogeneration system design for a high-tech science-based industrial park," *IEEE Trans. Industry Applications*, vol. 39, no. 5, pp. 1486-1492, 2003.

[10] *Electromagnetic Transients Program (EMTP), EMTP-V3 Rule Book I*, Development Coordination Group of EMTP, 1996.

[11] IEEE Standard 421.5, *IEEE Recommended Practice for Excitation System Models for Power System Stability Studies*, 2006.

[12] IEEE Committee Report, "Dynamic models for steam and hydro turbines in power system studies," *IEEE Trans. Power Apparatus and Systems*, 1973, vol. 92, pp. 1904-1915.

[13] Y. Li, H. D. Chiang, B. K. Choi, Y. T. Chen, D. H. Huang and M. G. Lauby, "Representative static load models for transient stability analysis: Development and Examination," *IET Gener. Transm. Distrib.*, vol. 1, (3), pp. 422–431, 2007.

[14] T. M. M. O'Flaherty and A. S. Aldred, "Synchronous-machine stability under asymmetrical faults," *Proceedings of the IEE - Part A: Power Engineering*, vol. 109, pp. 431-436, 1962.

Wei-Neng Chang was born in Tainan, Taiwan, ROC, in 1963. He received the B.Sc., M.Sc. and Ph.D. degrees from the National Taiwan University of Science and Technology, Taipei, Taiwan, in 1990, 1992, and 1996, respectively. He is now an associate professor with the Department of Electrical Engineering, Chang Gung University, Taiwan. He has been active in practical problems and has received more than 30 cooperative projects from electric power industry. His research interests include electric power quality, FACTS, power electronics, and DSP-based system designs and applications. He is a member of the IEEE since 1990.

Chia-Han Hsu was born in Taipei, Taiwan, ROC, in 1987. He received the B.Sc., and M.Sc. degrees from the Chang Gung University, Tao-Yuan, Taiwan, in 2009, and 2011, respectively. His research interest lies in electric power system engineering.